ELSEVIER

Desalination 234 (2008) 221–231

DESALINATION

www.elsevier.com/locate/desal

Embedded nano-iron polysulfone membrane for dehydration of the ethanol/water mixtures by pervaporation

Shih-Hsiung Chen[a]*, Rey-May Liou[a], Cheng-Lee Lai[a], Mu-Ya Hung[a], Mei-Hui Tsai[b], Shih-Liang Huang[b]

[a]*Department of Environmental Engineering and Science, Chia-Nan University of Pharmacy and Science, Tainan 717, Taiwan*

Tel. +886(7)2660028; Fax +886(6)266909; email: mshchen@mail.chna.edu.tw

[b]*Department of chemical and material Engineering, Chin-Yi University of Technology, Taichung, Taiwan*

Received 12 July 2007; accepted revised 28 September 2007

Abstract

Embedded nano-iron polysulfone membranes were prepared for dehydration of ethanol/water mixtures by pervaporation. It was found that the nano-iron particle can be prepared by in-situ thermal decomposition method in casting solution. The verification of the nano-particle dispersion in membrane was made by TEM measurement. It was found that the embedding nano-particle slightly increased the flux with the ordering polymer chains arrangement in membrane and also increased the separation factor. A remarkable enhancement in the separation factor of over 1000 can also be found in embedded membranes. But the flux of embedded membranes are lower (less than 350 g/m^2-h) than the flux of non-embedded polysulfone membranes (500 g/m^2-h). The increase in the separation factor of embedding membranes mainly contributed by the ordering/packing of polymer chains was caused by the surface effect of nano particle and limited the permeate diffusion behavior. On the other hand, it was found that the nano-particle embedding in the membrane showed a significant effect on the sorption behavior and presented a significant interaction between water and the embedded membrane. In this study, the high performance dehydration membranes were successfully prepared with nano-particle embedding in polysulfone membranes.

Keywords: Nano-iron; Polysulfone; Pervaporation; In-situ thermal decomposition

*Corresponding author.

Presented at the Fourth Conference of Aseanian Membrane Society (AMS 4), 16–18 August 2007, Taipei, Taiwan.

0011-9164/08/$– See front matter
doi:10.1016/j.desal.0000.00.000

1. Introduction

Nano-technologies based on novel systems associating metal particles to polymer matrix open a wide range of new applications [1–5]. The main goal for the addition of fillers to polymer focuses on the enhancement in the mechanical and electrical properties, heat resistance, and permeation barrier properties of polymers. The reinforcing ability of nano-additive depends on the particle size, structure, surface characteristics, and degree of dispersion in polymer matrix [6–8]. The permeation properties of polymer–clay nanocomposites based on organic polymers and inorganic clay minerals have already been discussed [9,10]. Recently, there are few studies concerning the association of nano-metal particles to polymeric membranes and their applications in separation processes.

It was expected that the addition of inorganic particles to membranes increased the permeability due to the disruption of polymer packing and lead to faster diffusion of penetrates in membranes. Contrarily, the inorganic nano-filler in membranes modified the polymer packing in matrix and led to a decrease in the penetrate diffusion and the flux of permeates [11–13]. Therefore, the characteristic of the nano-filler in membrane matrix plays an important role to determine the permeation behavior [14–18].

The purpose of this study is to investigate the effect of nano particles on the separation performance of composite membranes. The nano-iron particles were prepared by the in-situ thermal decomposition method in organic solvent (*N*-methyl-2-pyrrolidone, NMP). The morphology of nano-composite membranes was characterized by TEM images. The polymer packing and thermal properties were investigated by the thermal analysis. The separation performances of nano-composite membrane were characterized by pervaporation tests. The diffusion behavior and sorption properties of permeates were discussed by the sorption measurements and swelling tests.

2. Materials and methods

2.1. Materials

Udel® Polysulfone P-3500 was obtained from Amoco Performance Products. For membrane preparation, *N*-methyl-2-pyrrolidone (NMP) was used as the solvent. All chemicals and solvents used for the preparation of samples are reagent grade. For the preparation of nano-iron particles the carbonyl organometal ($Fe(CO)_5$) was used and thermally decomposed in NMP under inert atmosphere at 180°C [19–21]. After metallic particles were prepared in NMP solution, the casting solution was made with various iron contents for 24 stirrings before membrane preparation.

2.2. Membrane preparation

The nano-iron composite polysulfone membranes were prepared from a casting solution with varying iron content in NMP and membranes dry method at 80°C. The casting solution contained 25 wt.% polysulfone in NMP solution. With various amounts of nano-iron in casting solution, which was obtained from the thermal decomposition process, the solution was casted onto a glass plate to a predetermined thickness of 400 μm using a Gardner Knife. Then the casting film was kept in an oven for 2 h at 80°C. The dense membranes formed after 2 h and were peeled off. Finally, they were kept in a vacuum oven for 24 h before characteristics, sorption, and pervaporation measurements.

2.3. Pervaporation experiment

In pervaporation, the feed solution of 90 wt.% ethanol was in direct contact with the membrane and was kept at 25°C. The effective membrane area was 10.2 cm^2. The downstream pressure was maintained at about 5–8 Torr. The flux was determined by measuring the weights

of permeate [22–25]. The compositions of the feed solution permeate was measured by gas chromatography (GC, China Chromatography). The separation factor, $\alpha_{A/B}$, was calculated by the formula

$$\alpha_{A/B} = (Y_A/Y_B)/(X_A/X_B)$$

where, X_A, X_B and Y_A, Y_B are the weight fractions of A and B in the feed and permeate, respectively (A being the more permeative species).

2.4. Sorption measurements

The membranes were immersed in ethanol–water mixture for 24 h at 25°C. They were subsequently blotted between tissue papers to remove the excess solvent and then placed in the left half of a twin tube set-up. The system was evacuated while the tube was heated with hot water for 30 min and the right tube was cooled in liquid nitrogen. The composition of the condensed liquid in the right tube was determined by GC. The separation factor of sorption was calculated by

$$\alpha_{sorp} = (Y_w/Y_e)/(X_w/X_e)$$

where, X_e, X_w and Y_e, Y_w are the weight fractions of ethanol and water in the feed and membranes, respectively.

2.5. Swelling measurements

The degree of swelling of membranes were determined in distilled water and in aqueous ethanol solution at 25°C. The weight of dry membrane (W_{dry}) was first determined. After equilibrium with water or ethanol solution, the fully swollen membrane was wiped with tissue paper and weighed. Since the ethanol evaporated very fast, it was difficult to read the real weight directly. The weight of the membrane was measured every 5 s and plotted as a function of time for 30 s after wiping dry. The weight at time zero could be extrapolated and was taken as the swollen weight (W_{wet}) of the membrane. The degree of swelling was calculated by the following equation:

$$\text{Degree of swelling } (\%) = (W_{wet} - W_{dry})/W_{dry} \times 100\%$$

2.6. TEM and SEM studies

Surface morphology of the thoroughly dried membrane was studied by transmission electron microscopy (TEM) (Jeol-1400 transmission electron microscope). Hitachi S4100 SEM was used to observe the surface and cross-section structures of asymmetric membrane. In SEM studies, membrane samples were immersed in liquid nitrogen and then fractured for preparing samples. The SEM samples were then deposited with gold using a sputter coater.

2.7. Thermal analysis

MDA thermal analysis was performed using a Perkin-Elmer Pyris 7 DSC system. The measurements were made from 60 to 300°C, at a heating rate of 10°C min^{-1} in N_2 atmosphere. The sample size was about 5–10 mg.

2.8. IR spectra

All IR spectra were collected using 12 scans and 2 cm^{-1} resolution. The IR spectrum of each sample was obtained from a JASCO FT/IR 420.

3. Results and discussion

3.1. Morphology of composite membranes

For the purpose of clarifying the size of nano-iron in the composite membrane, the TEM

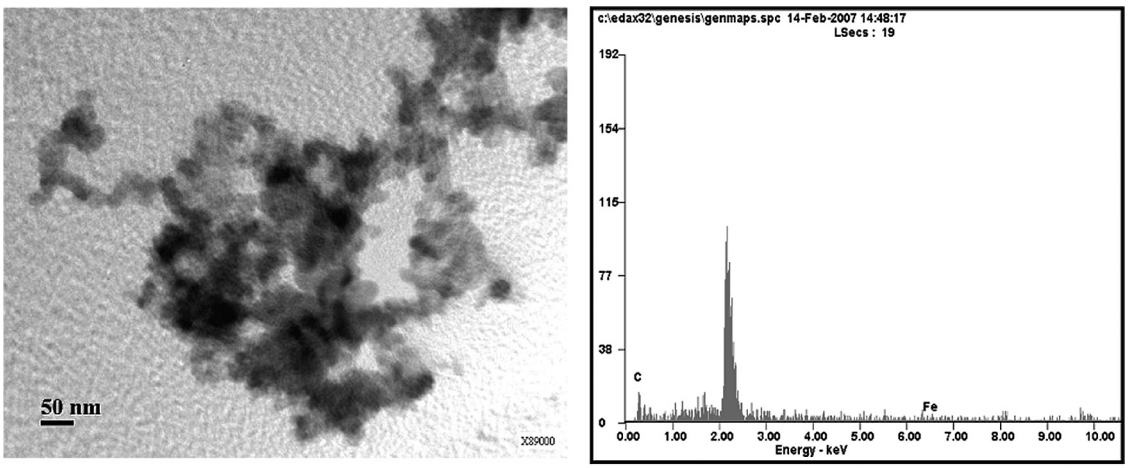

(A) (B)

Fig. 1. (A) TEM image (B) SEM-EDS of nano-composite membrane (8 wt.%).

images were made as shown in Fig. 1. It can be seen that less than 50 nm diameters of iron particles can be found in this TEM image. On the other hand, the SEM-EDS measurement was used for the elementary analysis to identify the iron content in membranes. It was found that the iron content in membranes were proportional to the adding ratio of metallic organic compounds in the membranes, though the EDS spectra is not shown in this paper. The results indicated that iron can be prepared by thermal decomposition method and is present in nano-size in polymer membranes. Similar results were also found in previous reports; the nano-particles embedded were identified by TEM technology in the polymer matrix [26,27].

3.2. Thermal properties of composite membranes

Fig. 2 shows the effect of nano-particle content on temperature profiles of DMA measurements. As shown in Fig. 2, the nano-particles embedded in the membrane increased the temperature of second Tan delta. It implied that more ordering polymeric packing was obtained with increasing the nano-particle content in membranes. It implies that the ordering/packing of polymer chains in composite membranes will affect their permeation behavior and selectivity.

3.3. IR spectra of composite membranes

Fig. 3 shows the FTIR spectra of nano-composite membranes which swelled in pure water. All the membranes had very similar spectra peaks at low wave numbers (650–2000 cm^{-1}). It can be seen that the carbonyl group existed in

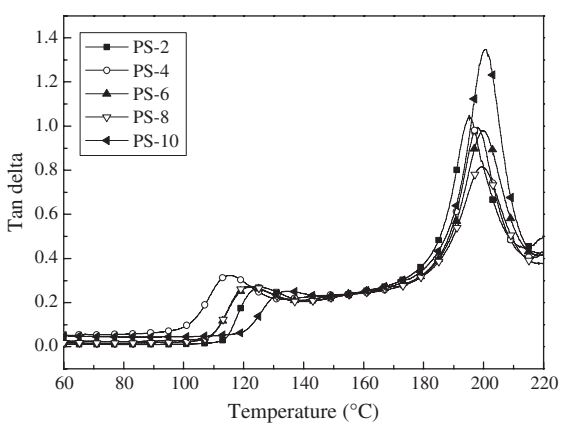

Fig. 2. DMA measurements of nano-composite membranes.

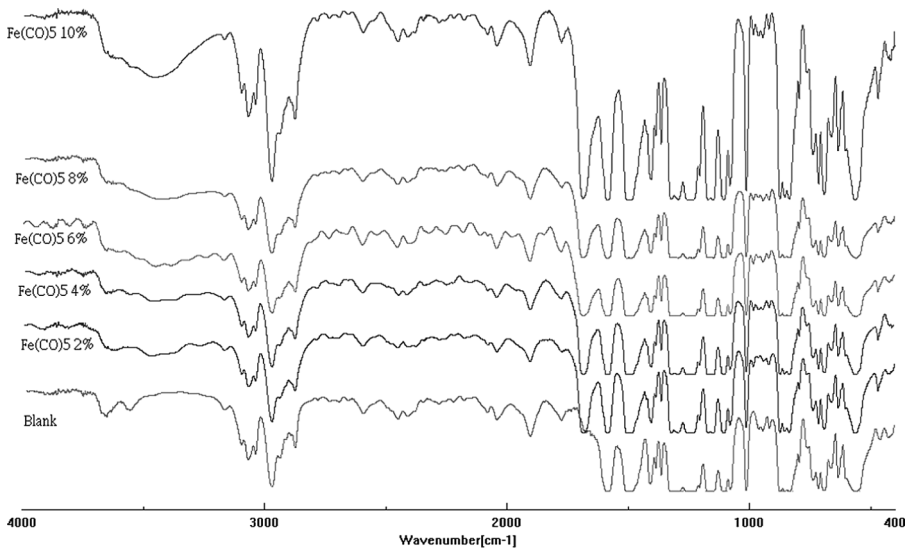

Fig. 3. FTIR spectra of iron nano-composite membranes with various nano-iron content.

the nano-composite membranes in the range of 2–10% iron content. All of the carbonyl groups did not show an increase in the intensity of absorbance, instead it showed that there was some unreactive metallic material in the composite membranes. It indicated that the unreacted metallic material was not proportional to the organic metallic reagent additive in the membranes. Therefore, it can be noted that there is some of the unreacted agent in the thermal decomposition procedure in 2 h reaction. On the other hand, the wave number of 3400–3600 cm^{-1} is the OH bond of the sorption water in membranes [28,29]. It can be seen that the broad band around this range shifted to a low wave number with increasing the embedding iron in the composite membranes. The shift of the wave number indicated that the water molecule was affected by the interaction force in the membrane. It was proposed that some hydration force was formed around the iron surface due to oxidation of the iron. The hydration of metal oxide usually can be found in an aqueous solution.

The vs 3400–3600 cm^{-1} is a band of water molecules in the composite membranes and the shift of the wave number was due to the interaction between water and polymer in the membranes. Therefore, it indicates that the embedding of nano-iron strongly shifted the band to a higher wave number. It also implied that the strong shift showed an increased interaction of water molecules in the membrane. Thus it can be expected that the sorption selectivity of embedding membrane increased the selectivity of water to ethanol in test conditions.

3.4. Separation performance of composite membranes

Fig. 4 shows the effect of embedding nano-iron on the separation performance of composite membranes. It can be seen that the flux slightly increased with increasing the nano-particle content in composite membranes. However, the flux of embedded membranes with low iron content is lower than the pure polysulfone membrane (22). It was indicated that the embedding iron significantly decreased the flux with high-order polymer packing in membranes and it was coincided with the result of DMA tests. It was

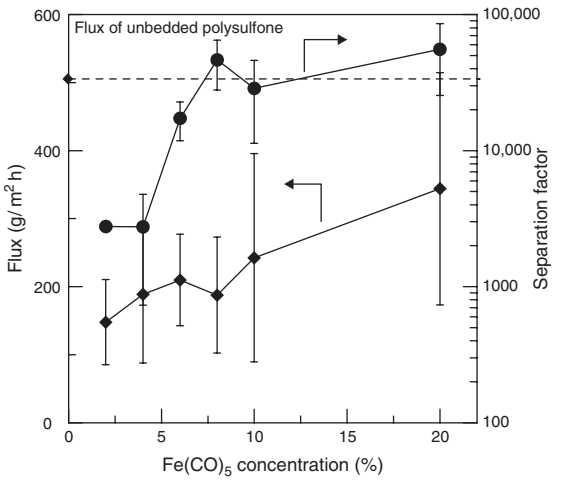

Fig. 4. Effect of nano-particle content on the pervaporation properties of composite membranes.

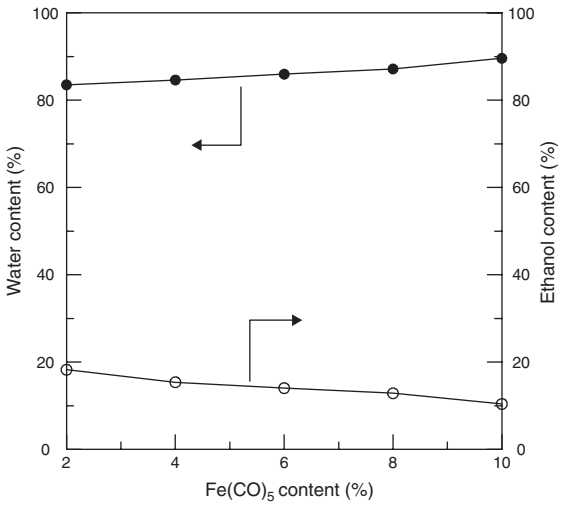

Fig. 5. Sorption tests of nano-iron embedded membranes in the 90 wt.% ethanol solution.

proposed that the embedding nano-particle increased the polymer packing in composite membranes and significantly decreased the permeation rate. On the other hand, the separation factor of composite membranes rapidly increased. The increase in the separation factor may be contributed by the increase in diffusion selectivity or sorption selectivity of the embedded membranes which was caused by the embedded nano-iron.

It is interesting to note that the increase of iron content in membranes enhanced both the flux and separation factor of nano-iron embedded membranes. Generally, the modification of additive technology induced two possible effects on the membrane matrix [30]. The first one is that the additive material induced a close packing between the membrane matrix and the additive. In this case, the dense structure of modified membrane owns a low flux and enhances the separation factor. The other one is that the additional material presented the low compatibility in polymer matrix and induces phase separation in membrane matrix. Therefore, those phase separations of modified membrane induced a loss of separation factor and an increase in the flux of membranes [31,32]. In this study, the embedded membranes showed different results to the above cases. Therefore, more experiments must be made to distinguish the effect of nano-particles embedded in the polymer membrane on the increase in both the flux and the separation factor.

The sorption test of nano-iron embedded membranes for the 90 wt.% ethanol solution is shown in Fig. 5. It can be seen that the water content in membranes increased with increasing the nano-iron content. It can also be seen that water is a preferable adsorbed permeate than the ethanol in membranes and the water content in membranes is proportional to the increasing in nano-iron particle content. It shows that the composite membranes with nano-iron particles embedded may change the hydrophilicity of membranes. However, it should be noted that the polymer and nano iron are hydrophobic material and there is no possibility to enhance the hydrophilic properties of composite membranes. Thus, the hydration of iron is one of the possible reasons to change the hydrophilic property of embedded membranes. It should also be noted that nano-iron easily oxidises in air and forms iron oxides. The hydration of iron oxides

is easy in an aqueous solution. Therefore, the oxidation of metal may play an important role in the change of the membranes' hydrophilicity.

As shown in Fig. 4, the separation factor of iron embedded membranes increased with an iron content of up to 8% and then slightly decreased with more iron embedded in the membranes. On the other hand, the flux of those membranes increased with the iron content in the composite membranes. The pervaporation separation index (PSI) is the product of the total flux and separation factor, and it is a good index for determining the performance of a pervaporation membrane. Fig. 6 show the dependence of PSI of composite membranes on the amount of iron embedding. It can be seen that the PSI value increased as the iron content was increased up to 8% but the embedded 10% iron content in the membrane presents a large standard deviation because of the poor distribution of nano-iron particles in the membrane. Thus, it is proposed that a higher content of nano-iron lead to a poor membrane formation, and therefore the PSI value showed a large standard deviation with increasing iron content in membranes (when the iron content was larger than 10%). The PSI values were contributed by both flux and separation factor, and the small difference in the flux indicates that the change of PSI value was due to the difference flux of permeate in the modified membranes.

To further distinguish the reason that caused the change of PSI, the effect of iron-embedded content on the sorption and diffusion properties should be discussed in modified membranes. The diffusion selectivity (α^{d}) can be defined as the ratio of permeation selectivity (α^{p}) and sorption selectivity (α^{s}) [33]:

$$\alpha^{p} = \alpha^{d}\,\alpha^{s}$$

Based on the permeation data and the sorption measurements, permeation selectivity (α^{p}) and sorption selectivity (α^{s}) can be obtained. Fig. 7 show the relationship between diffusion selectivity and iron content in embedded membranes. It can be seen that the sorption selectivity increased with increasing nano-iron content in the composite membranes. It can also be seen that the diffusion separation factor is much more than the sorption separation factor. As shown in Fig. 4, the separation factor first increased with

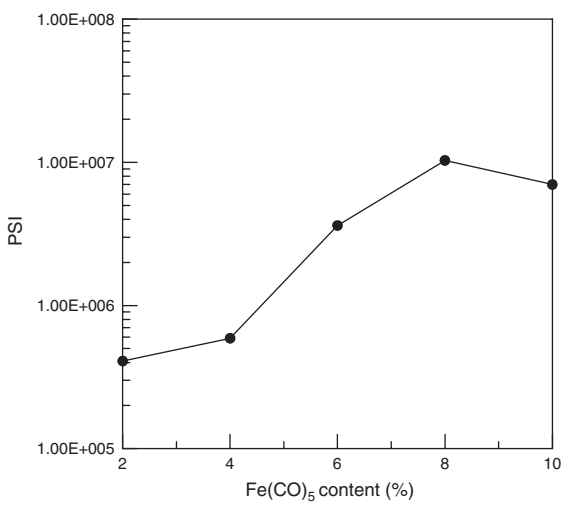

Fig. 6. Effect of nano-particle content on the pervaporation standard index of composite membranes.

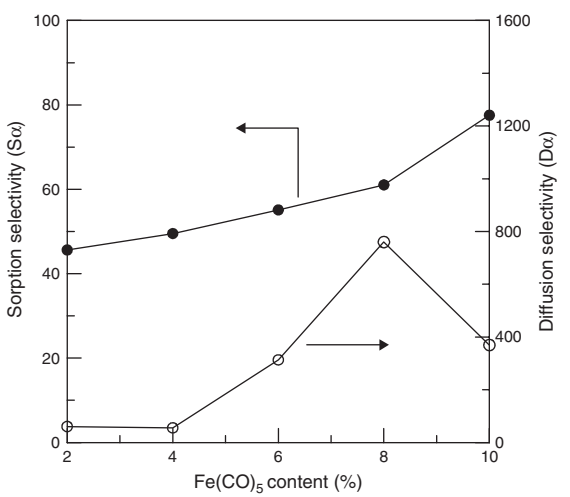

Fig. 7. Effect of nano-particle content on the sorption and diffusion properties of composite membranes.

increasing nano-iron content in composite membranes (up to 8%), and then slightly decreased, indicating that the dominant influence on the separation factor was permeate diffusion behavior. It can also be seen that the diffusion selectivity first increased with up to 8% of nano-iron content and then decreased to 10% iron content in the membranes, implying that a loose packing density of the composite membrane was formed.

To further distinguish the enhancement of hydrophilicity by embedding nano-iron, the swelling test of different iron contents with 90% ethanol in the feed were made. Fig. 8 shows the effect of different iron contents on the degree of swelling of embedded membrane. It can be seen that the degree of swelling slightly increased as the nano-iron content in the composite membranes increased at 90% ethanol composition in feed. The larger swelling properties at high iron content implied that the membrane structure would be loose membrane

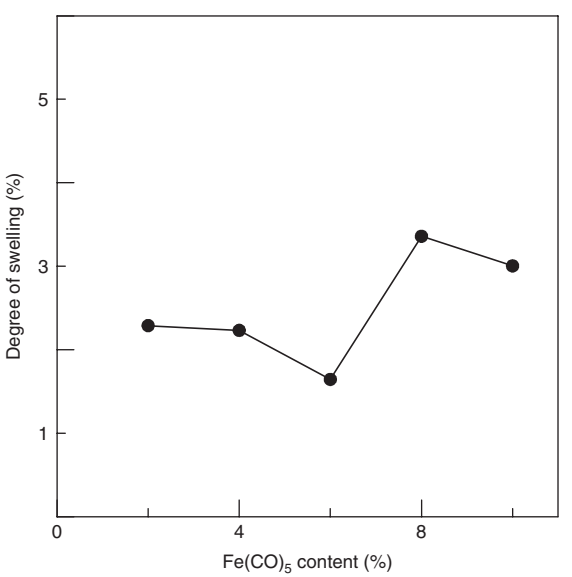

Fig. 8. Effect of nano-particle content on the degree of swelling of composite membranes.

packing due to the swelling of polymer chain by absorbing more permeates in membranes. A lower packing density of membrane usually leads to decreased diffusion selectivity in the pervaporation process.

However, Fig. 7 shows the relationship between iron content in membranes and sorption selectivity of composite membranes, indicating that the sorption selectivity increased with increasing iron content in membranes. The loose polymer packing lead to a coupling effect and resulted in a decrease in separation factor. However, the embedded membranes did not decrease the separation factor of membranes. It was proposed that the enhancement of water adsorption in membranes, which swelled the polymer chain, was contributed by hydration of embedded iron oxides in membranes.

On the other hand, it can be seen that the diffusion selectivity first increased with increasing the iron content and then decreased after 8 wt.%. This behavior did not coincide with the result of the swelling measurement. It indicated that in the nano-iron embedded in membrane matrix an interaction exists between nano-iron and polymer. However, the nano-particle embedded in the membrane enhanced the hydrophilic properties and induced an increase in the sorption selectivity of membranes. The iron oxidation was supposed to be the major factor to induce this phenomenon. There are evidences that the iron will be quickly oxidised in air to form iron oxides [34,35]. The evidence for this study to identify the oxidation of nano-iron in membranes will be provided in the future works and the effect of oxidation of nano-iron on the hydration will also be discussed. In this investigation, the increase in swelling induced a flexible polymer chain in iron embedded membranes. Therefore, the swelling effects decreased the diffusion selectivity of membranes with the iron content at 10% and with too much swelling permeate in membranes.

3.5. Effect of operating temperature on pervaporation properties

Fig. 9 shows the effect of feed temperature on permeation flux and separation factor of iron-embedded membrane with 90% ethanol in feed solution. It can be seen that the permeation flux increased with increasing feed temperature, while the separation factor decreased with increasing the operating temperature. It is well known that the decrease of separation factor was due to the increase of molecular motion with increasing the feed temperature. The increase in permeation flux with operating temperature in feed was due to the increase in membrane swelling.

As shown in Fig. 9, less flux was found at 25°C and the separation factor shows the same proportion to iron content. However, the flux slightly decreased with increasing nano-iron content in membranes at 45°C and the separation factor was almost constant at 45°C, which was still larger than 1500 for all composite membranes. Generally, the amount of liquid absorbed into a solid membrane typically increased with increasing temperature. On the other hand, the chain mobility of polymer membranes also increased with increasing operating temperatures. A swelling membrane could be formed by increasing the chain mobility and permeate sorption in membrane. Therefore, an increase in permeation flux with increased temperature will be found.

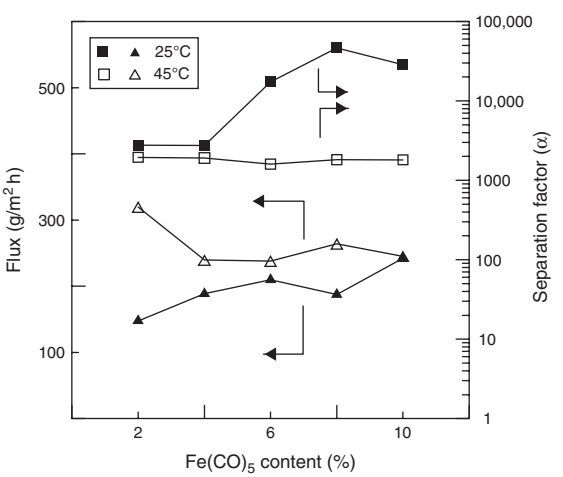

Fig. 9. Effect of operating temperature on the permeation properties of composite membranes.

4. Conclusion

Embedded nano-iron polysulfone membranes were successfully prepared for dehydration of ethanol/water mixtures by pervaporation. It was found that the nano-iron particle can be prepared with in-situ thermal decomposition method in casting solution. The TEM observation verified the nano-particle in the composite membranes. It was found that the embedding nano-particle slightly increased the flux of membrane and strongly increased the separation factor due to the interaction between nano-iron and polymer in membranes. The embedded iron in composite membranes showed an obvious effect on the permeation and sorption behaviors of embedding membranes. It is proposed that nano iron affected the ordering/packing of polymer chains and some of the particle oxide, which influenced the hydrophilic prosperity. Then, it was found that the nano-particle embedding in membrane showed a significant effect on the sorption behavior and the interaction between water molecules and the membrane. In this study, the high performance dehydration membranes were successfully prepared with nano-particle embedding in glassy polymeric membranes.

Acknowledgements

The authors thank the National Science Council of Republic of China (NSC-93-2216-E-041-003), Taiwan, R.O.C. for their financial support in this research. The authors also thank the Center-of-Excellence Program on Membrane Technology, the Ministry of Education,

Taiwan, R.O.C. for their financial and technology support in this research.

References

[1] F.-K. Liu, S.-Y. Hsieh, F.-H. Ko and T.-C. Chu, Synthesis of gold/poly(methyl methacrylate) hybrid nanocomposites, Colloids Surf. A, 231 (2003) 31–38.

[2] P. Lijiaa, D. Chen, P. He, X. Zhu, L. Weng, Alternative method for preparation of CdS/epoxy resin nanocomposite, Materials Research Bulletin, 39 (2004) 243–249.

[3] R. Yu, H.-Z. Chen, G. Wu and M. Wang, Preparation and characterization of titanium dioxide nanoparticle/polystyrene composites via radical polymerization, Mater. Chem. Phys., 91 (2005) 370–374.

[4] C. Pichot, Surface-functionalized latexes for biotechnological applications, Curr. Opin. Colloid Interface Sci., 9 (2004) 213–221.

[5] Z. Varga, G. Filipcsei and M. Zrı′nyi, Smart composites with controlled anisotropy, Polymer, 46 (2005) 7779–7787.

[6] C. Yilmaz and T. Korkmaz, The reinforcement effect of nano and microfillers on fracture toughness of two provisional resin materials, Mater. Design, 28 (2007) 2063–2070.

[7] J. Zeng, B. Saltysiak, W.S. Johnson, D.A. Schiraldi and S. Kumar, Processing and properties of poly(methyl methacrylate)/carbon nano fiber composites, Composites: Part B, 35 (2004) 173–178.

[8] C. Takai, M. Fuji and M. Takahashi, A novel surface designed technique to disperse silica nano particle into polymer, Colloids Surf. A: Physicochem. Eng. Aspects, 292 (2007) 79–82.

[9] R. Stephen, C. Ranganathaiah, S. Varghese, K. Joseph and S. Thomas, Gas transport through nano and micro composites of natural rubber (NR) and their blends with carboxylated styrene butadiene rubber (XSBR) latex membranes, Polymer, 47 (2006) 858–870.

[10] S. K. Chakarvarti and J. Vetter, Template synthesis — A membrane based Technology for generation of nano-/micro material: a review, Radiat. Meas., 29 (1998) 149–159.

[11] M.H. Cho and S. Bahadur, Study of the tribological synergistic effects in nano CuO-filled and fiber-reinforced polyphenylene sulfide composites, Wear, 258 (2005) 835–845.

[12] S. Bahadur and C. Sunkara, Effect of transfer film structure, composition and bonding on the tribological behavior of polyphenylene sulfide filled with nano particles of TiO_2, ZnO, CuO and SiC, Wear, 258 (2005) 1411–1421.

[13] S. I. Marras, I. Zuburtikudis and C. Panayiotou, Nanostructure vs. microstructure: morphological and thermomechanical characterization of poly-(L-lactic acid)/layered silicate hybrids, Eur. Polym. J., 43 (2007) 2191–2206.

[14] T.C. Merkel, Z. He, I. Pinnau, B.D. Freeman, P. Meakin and A.J. Hill, Effect of nanoparticles on gas sorption and transport in Poly(1-trimethylsilyl-1-propyne), Macromolecules, 36 (2003) 6844–6855.

[15] Z. He, I. Pinnau and A. Morisato, Nanostructured poly(4-methyl-2-pentyne)/silica hybrid membranes for gas separation, Desalination, 146 (2002) 11–15.

[16] B.H.B. Bouma, A. Checchetti, G. Chidichimo and E. Drioli, Permeation through a heterogeneous membrane: the effect of the disperse phase, J. Membr. Sci., 128 (1997) 141–149.

[17] S. Kumar, J.N. Shah, S.B. Sawant, J.B. Joshi and V.G. Pangarkar, Permeation in filled membranes: role of solute-filter interaction, J. membr. Sci., 134 (1997) 225–233.

[18] C.K. Chung, P.K. Fung, Y.Z. Hong, M.S. Ju, C.C.K. Lin and T.C. Wu, A novel fabrication of ionic polymer-metal composites (IPMC) actuator with silver nano-powders, Sens. Actuators B, 117 (2006) 367–375.

[19] D. Mahajan, A. Desai, M. Rafailovich, M.-H. Cui and N.-L. Yang, Synthesis and characterization of nanosized metals embedded in polystyrene matrix, Composites: Part B, 37 (2006) 74–80.

[20] H Li, M. Eddaoudi, M. O'Keeffe and O.M. Yaghi, Design and synthesis of an exceptionally stable and highly porous metal-organic network. Nature, 402 (1999) 276–279.

[21] T.W. Smith and D. Wychick, Colloidal dispersions prepared via the polymer-catalyzed decomposition of iron pentacarbonyl, J. Phys. Chem., 84 (1980) 1621–1629.

[22] S.-H. Chen, R.M. Liou, C.-S. Hsu and K.-C. Yu, Pervaporation separation water/ethanol mixture through lithiated polysulfone membrane, J. Membr. Sci., 193 (2001) 59–67.

[23] S.-H. Chen, K.-C. Yu, S.-S. Lin, D. J. Chang and R.M. iou, Pervaporation separation of water/ethanol mixture by sulfonated Polysulfone membrane, J. Membr. Sci., 183 (2001) 29–36.

[24] C.-S. Hsu, S.-H. Chen, R.-M. Liou, M-Y. Hung, H.A. Tsia and J.-Y. Lai, Pervaporation separation of water/ethanol mixture by PSF/PEG blending membrane, J. Appl. Polym. Sci., 87 (2003) 2158–2164.

[25] M.-Y. Hung, S.-H. Chen, C.-S. Hsu, R.-M. Liou, H.A. Tsia and J.-Y. Lai, Pervaporation separation of water/ethanol mixture by polysulfone/plasticizer blending membrane, Eur. polym. J., 39 (2003) 2367–2374.

[26] T. Yu, J. Lin, J. Xu, T. Chen and S. Lin, Novel polyacrylonitrile nanocomposites containing Na-montmorillonite and nano SiO_2 particle, Polymer, 46 (2005) 5695–5697.

[27] D. Mahajan, A. Desai, M. Rafailovich, M.-H. Cui and N.-L. Yang, Synthesis and characterization of nanosized metals embedded in polystyrene matrix, Composites: Part B, 37 (2006) 74–80.

[28] T. Hiemstra and W.H.V. Riemsdijk, On the relationship between charge distribution, surface hydration, and the structure of the interface of metal hydroxides, J. Colloid Interface Sci., 301 (2006) 1–18.

[29] H. Tamura, K. Mita, A. Tanaka and M. Ito, Mechanism of hydroxylation of metal oxide surfaces, J. Colloid Interface Sci., 243 (2001) 202–207.

[30] A. Li, W. Liang and R. Hughes, Repair of a Pd/a-Al_2O_3 composite membrane containing defects, Sep. Purif. Technol., 15 (1999) 113–119.

[31] J. Huang and M.M. Meagher, Pervaporative recovery of *n*-butanol from aqueous solutions and ABE fermentation broth using thin-film silicalite-filled silicone composite membranes, J. Membr. Sci., 192 (2001) 231–242.

[32] C.M. Braunbarth, L.C. Boudreau and M. Tsapatsis, Synthesis of ETS-4/TiO_2 composite membranes and their pervaporation performance, J. Membr. Sci., 174 (2000) 31–42.

[33] R.Y.M. Huang, Pervaporation Separation Process, Elsevier Science Publishers B. V., 1991.

[34] X.Y. Qin, J.G. Kim and J.S. Lee, Synthesis and magnetic properties of nanostructured g-Ni-Fe alloys, Nano Struct. Mater., 11 (2) (1999) 259–270.

[35] A.J. Feitz, S.H. Joo, J. Guan, Q. Sun, D.L. Sedlak and T.D. Waite, Oxidative transformation of contaminants using colloidal zero-valent iron, Colloids Surf. A: Physicochem. Eng. Aspects, 265 (2005) 88–94.